






Article

Point-Substitution of Phenylalanine Residues of 26RFa Neuropeptide: A Structure-Activity Relationship Study

Benjamin Lefranc^{1,2,†}, Karima Alim^{1,†}, Cindy Neveu^{1,†}, Olivier Le Marec^{1,†}, Christophe Dubessy^{1,2}, Jean A. Boutin^{3,4}, Julien Chuquet¹, David Vaudry^{1,2}, Gaëtan Prévost¹, Marie Picot¹, Hubert Vaudry^{1,2}, Nicolas Chartrel¹ and Jérôme Leprince^{1,2,*}

- ¹ INSERM U1239, Laboratory of Neuronal and Neuroendocrine Differentiation and Communication, Normandy University, 76000 Rouen, France; benjamin.lefranc@univ-rouen.fr (B.L.); alimkarima8@gmail.com (K.A.); duchemin@neurofit.com (C.N.); lemarec.olivier@gmail.com (O.L.M.); christophe.dubessy@univ-rouen.fr (C.D.); julien.chuquet@univ-rouen.fr (J.C.); david.vaudry@univ-rouen.fr (D.V.); gaetan.prevost@chu-rouen.fr (G.P.); marie.picot@univ-rouen.fr (M.P.); hubert.vaudry@univ-rouen.fr (H.V.); nicolas.chartrel@univ-rouen.fr (N.C.)
- ² Cell Imaging Platform of Normandy, PRIMACEN, Normandy University, 76000 Rouen, France
- ³ Institut de Recherches Internationales SERVIER, 50 rue Carnot, 92284 Suresnes, France; ja.boutin.pro@gmail.com
- ⁴ PHARMADEV, Faculté de Pharmacie, Université de Toulouse, 31062 Toulouse, France
- * Correspondence: jerome.leprince@univ-rouen.fr; Tel.: +33-235-14-6132
- † These authors equally contributed to this work.



Citation: Lefranc, B.; Alim, K.; Neveu, C.; Le Marec, O.; Dubessy, C.; Boutin, J.A.; Chuquet, J.; Vaudry, D.; Prévost, G.; Picot, M.; et al. Point-Substitution of Phenylalanine Residues of 26RFa Neuropeptide: A Structure-Activity Relationship Study. *Molecules* **2021**, *26*, 4312. <https://doi.org/10.3390/molecules26144312>

Academic Editor:
Katalin Prokai-Tatrai

Received: 7 June 2021
Accepted: 12 July 2021
Published: 16 July 2021

Publisher's Note: MDPI stays neutral with regard to jurisdictional claims in published maps and institutional affiliations.



Copyright: © 2021 by the authors. Licensee MDPI, Basel, Switzerland. This article is an open access article distributed under the terms and conditions of the Creative Commons Attribution (CC BY) license (<https://creativecommons.org/licenses/by/4.0/>).

Abstract: 26RFa is a neuropeptide that activates the rhodopsin-like G protein-coupled receptor QRFP/R/GPR103. This peptidergic system is involved in the regulation of a wide array of physiological processes including feeding behavior and glucose homeostasis. Herein, the pharmacological profile of a homogenous library of QRFP-targeting peptide derivatives was investigated in vitro on human QRFP-transfected cells with the aim to provide possible insights into the structural determinants of the Phe residues to govern receptor activation. Our work advocates to include in next generations of 26RFa_(20–26)-based QRFP agonists effective substitutions for each Phe unit, i.e., replacement of the Phe²² residue by a constrained 1,2,3,4-tetrahydroisoquinoline-3-carboxylic acid moiety, and substitution of both Phe²⁴ and Phe²⁶ by their *para*-chloro counterpart. Taken as a whole, this study emphasizes that optimized modifications in the C-terminal part of 26RFa are mandatory to design selective and potent peptide agonists for human QRFP.

Keywords: GPR103; QRFP; RFamide; intracellular calcium concentration; peptide analog

1. Introduction

The neuropeptides 26RFa (QRFP26) and its N-terminal extended form 43RFa (QRFP, Figure 1) are the endogenous ligands of the G_{i/s/q} coupled QRFP receptor (QRFP), formerly known as the orphan receptor GPR103 [1–3]. Since the isolation of 26RFa from a European green frog *Rana esculenta* brain extract [4], prepro-26RFa cDNA has been characterized in numerous genomes of diverse vertebrates from fish to mammals [5]. However, very few mature peptides have been identified so far, leaving the 26RFa/QRFP precursor post-translational processing uncertain. Indeed, in avians, 26RFa orthologs have been isolated and sequenced from the Japanese quail [6] and zebra finch [7] while, in rodents, only the 43RFa counterpart has been characterized from rat [2,8]. In humans, both 26RFa- and 43RFa-immunoreactive forms have been detected in hypothalamic and spinal cord extracts [9]. Interestingly, the presence of a tribasic cleavage site (Arg-Lys-Arg/Lys) within the 26RFa sequence suggests that the C-terminal heptapeptide GGFSFRF-NH₂, named 26RFa_(20–26), could also be produced from the precursor. However, to date, this fragment, whose sequence is highly conserved in tetrapods, has not been identified as a mature product of the 26RFa/QRFP gene transcription.

Human 26RFa:

TSGPLGNLAEELNGYSRKKGGFSFRF-NH₂

Human 43RFa:

<EDEGSEATGFLPAAGEKTSGPLGNLAEELNGYSRKKGGFSFRF-NH₂

Figure 1. Primary structures of human 26RFa and 43RFa/QRFP. <E denotes pyroglutamic acid.

In rats, the 26RFa/QRFP gene is primarily expressed in hypothalamic neurons which project in various brain areas [1,2,8,10]. Consistent with the widespread distribution of 26RFa/QRFP-containing fibers, 26RFa and/or QRFP are involved in the regulation of multiple physiological activities [5]. In particular, it is now firmly established that 26RFa and QRFP stimulate food intake in rodents [1,8,10–16]. There is also evidence that 26RFa and/or QRFP regulate several other neuroendocrine and cognitive functions including reproduction [17,18], anxiety [19], memory [20], cardiovascular activity [8] and nociceptive transmission [21–23], some of which depend, at least in part, on off-target interaction with QRFP-related receptors [24,25]. In addition, recent data reveal that the 26RFa/QRFP system controls glucose homeostasis at the periphery by increasing insulin sensitivity and inhibiting hepatic glucose production [26–29]. Thus, QRFP represents an attractive target for the development of innovative drugs. Indeed, there is now clinical evidence for possible indications of QRFP ligands for the treatment of metabolic disorders, obesity and diabetes [5].

As a molecular signature, the RF-amide C-terminal extremity of 26RFa/QRFP and other RF-amide-related peptides (i.e., NPAF/NPFF, PrRP, RFRP-1(GnIH)/RFRP-3 and kisspeptin in humans [30]) represents the chemical determinant for bioactivity. Notably, deamidation or local side-chain substitution of the RF-amide moiety is generally associated with full or partial loss of activity and/or affinity of these neuropeptides [2,31–33]. The N-terminal part of RF-amide-related peptides diverges in their sequence and length, and conditions the whole or partial affinity and selectivity for one or several receptors, respectively [34,35]. For instance, 26RFa also binds with nanomolar affinity to both NPFF1 and NPFF2 receptors [24]. However, 26RFa can be downsized from the N-terminal extremity with a gradual decrease in its ability to mobilize intracellular calcium concentration ($[Ca^{2+}]_i$) in CHO cells transfected by the human QRFP (*hQRFP*) [36]. Since 26RFa_(20–26) (LV-2021) mimics the orexigenic and gonadotropic effects of full-length 26RFa [12,17], it appears that this C-terminal heptapeptide can serve as a molecular scaffold for designing low molecular weight, potent and stable *hQRFP* ligands. As a matter of fact, 26RFa_(20–26) has already been successfully used to design nanomolar active agonists such as [Nva²³]26RFa_(20–26) (LV-2073) [36], [Cmp²¹, aza-β³-Hht²³]26RFa_(21–26) (LV-2172) [37], and [(Me)^ωArg²⁵]26RFa_(20–26) (LV-2186) [38], as well as proteolytic resistant pseudopeptides (Figure 2) [39]. According to our previous structure-activity relationship studies [for review, 5], these compounds exhibit modifications at positions occupied by residues classified as permissive to substitution or engaged in peptide bonds susceptible to degradation. In contrast, the residues of the -Phe²⁴-Arg²⁵-Phe²⁶-NH₂ triad are very sensitive to substitutions and only tolerate subtle amendments for improving bioactivity like the ω-methylation of arginine 25 [38]. To date, few replacements have been reported in the phenylalanine positions of 26RFa_(20–26) [5]. As previously suggested for PrRP and kisspeptin [40], our work emphasizes that optimized modifications in the C-terminal part of 26RFa are mandatory to design selective and potent peptidergic ligands for *hQRFP*.

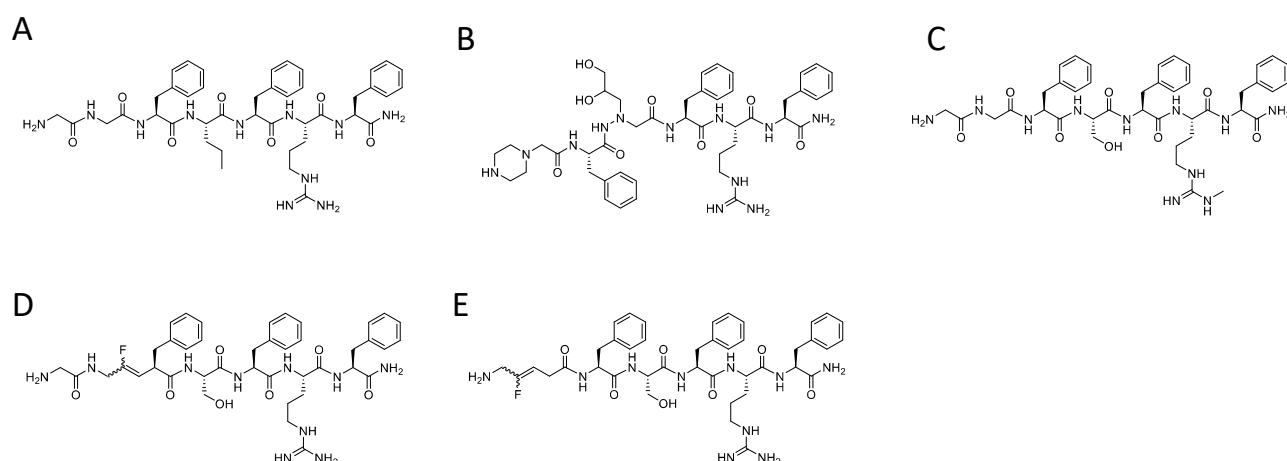


Figure 2. Chemical structures of peptidic and pseudopeptidic human QRFPR ligands. (A) [Nva²³]26RFa_(20–26) (LV-2073); (B) [Cmpi²¹, aza-β³-Hht²³]26RFa_(21–26) (LV-2172); (C) [(Me)^ω Arg²⁵]26RFa_(20–26) (LV-2186); (D) [ψ(CF=CH)^{21,22}]26RFa_(20–26); (E) [ψ(CF=CH)^{20,21}]26RFa_(20–26).

Thus, the aim of the present study was to investigate molecular diversity at the unexplored Phe positions to go deeper into the structure-activity relationships of 26RFa for the design of potent *h*QRFPR agonists.

2. Results and Discussion

2.1. Impact of Modifications of Each Phenylalanine Residue

It is well-accepted that the (hetero)aromatic units of peptides and proteins are master residues for DNA recognition [41], folding [42] and receptor-ligand interaction [43]. In particular, His, Phe, Trp and Tyr contribute to three types of non-covalent interactions including π -hydrogen bonds, electrostatic cation- π interactions and van der Waals π - π interactions [44] for governing molecular recognition of a ligand into the binding site of the receptor and transduction processes.

Replacement of all three phenylalanine residues of 26RFa_(20–26) (LV-2021, **1**) with an alanine moiety identifies Phe²⁴ and Phe²⁶ as key residues for QRFPR activation, unlike Phe²² which is rather permissive to this substitution and thus weakly participates in the activity of the peptide [36]. Accordingly, Phe²⁴ and Phe²⁶ side chains strongly interact with hydrophobic regions at the bottom of the binding pocket of the *h*QRFPR homology model [45]. In order to optimize positions 22, 24 and 26 of LV-2021, we have successively replaced each phenylalanine of the heptapeptide **1** with different commercially available aromatic or aliphatic building blocks (Table 1, compounds 2–48) and evaluated their ability to mobilize [Ca²⁺]_i in cultured G_{α16}-*h*QRFPR-transfected CHO cells (Table 2), as previously described [36]. Substitution with the isosteric residue 3-(2-thienyl)-alanine (Thi) yielded compounds LV-2050, LV-2051 and LV-2052 (**2–4**) that were less active than the parent peptide whatever the position concerned (Table 2). Similarly, incorporation of more hindered residues such as 3-(2-naphthyl)-alanine (2Nal; LV-2065, LV-2213, LV-2191, **5–7**) and tryptophane (LV-2210, LV-2204, LV-2187, **8–10**) altered the agonistic activity of the compounds, suggesting that there was little space available at the bottom of the orthosteric binding site as previously reported [45]. However, the para position of the Phe²⁶ residue tolerated a bulky group or a substituent with different electronic effects. Indeed, [*pt*BuPhe²⁶]26RFa_(20–26) (LV-2238, **13**), [Pcp²⁶]26RFa_(20–26) (LV-2193, **16**) and [*p*NO₂Phe²⁶]26RFa_(20–26) (LV-2194, **19**) were significantly more potent than 26RFa_(20–26) (LV-2021, **1**) to increase [Ca²⁺]_i in vitro (Table 2, Figure 3A–C). The same substitutions at positions Phe²² and Phe²⁴ were either neutral (**15**, **17**) or deleterious to activity (**11**, **12**, **14**, **18**). Finally, methylene shortening of the phenylalanine side chain led to the inactive phenylglycine (Phg)-containing [Phg²²]26RFa_(20–26) (LV-2053, **20**), [Phg²⁴]26RFa_(20–26) (LV-2054, **21**; LV-2055, **22**) and [Phg²⁶]26RFa_(20–26) (LV-2056, **23**; LV-2057, **24**) diastereoisomers, probably

due to the lack of interactions with hydrophobic residues in the core of the *h*QRFP binding pocket.

Table 1. Chemical data for 26RFa_(20–26) analogs substituted in positions 22, 24 and 26.

Peptide	Structure of Residue 22, 24, 26	Code	HPLC		MS	
			Rt (min) ^a	Purity (%)	Calcd ^b	Obsd ^c
1	26RFa _(20–26)	LV-2021	18.0	99.9	815.41	816.53
2	[Thi ²²]26RFa _(20–26)	LV-2050	18.6	99.9	821.36	822.33
3	[Thi ²⁴]26RFa _(20–26)	LV-2051	18.6	99.9	821.36	822.37
4	[Thi ²⁶]26RFa _(20–26)	LV-2052	18.6	99.9	821.36	822.38
5	[2Nal ²²]26RFa _(20–26)	LV-2065	20.4	99.9	865.42	866.45
6	[2Nal ²⁴]26RFa _(20–26)	LV-2213	20.8	99.9	865.42	866.46
7	[2Nal ²⁶]26RFa _(20–26)	LV-2191	20.6	99.9	865.42	866.57
8	[Trp ²²]26RFa _(20–26)	LV-2210	18.9	99.9	854.42	855.27
9	[Trp ²⁴]26RFa _(20–26)	LV-2204	18.6	99.9	854.42	855.43
10	[Trp ²⁶]26RFa _(20–26)	LV-2187	19.3	99.9	854.42	855.48
11	[<i>pt</i> BuPhe ²²]26RFa _(20–26)	LV-2068	22.1	99.9	871.47	872.49
12	[<i>pt</i> BuPhe ²⁴]26RFa _(20–26)	LV-2235	22.3	99.9	871.47	872.45
13	[<i>pt</i> BuPhe ²⁶]26RFa _(20–26)	LV-2238	22.4	99.9	871.47	872.55
14	[Pcp ²²]26RFa _(20–26)	LV-2069	19.9	99.9	849.37	850.30
15	[Pcp ²⁴]26RFa _(20–26)	LV-2232	20.5	99.9	849.37	850.41
16	[Pcp ²⁶]26RFa _(20–26)	LV-2193	20.0	99.9	849.37	850.42
17	[<i>p</i> NO ₂ Phe ²²]26RFa _(20–26)	LV-2214	19.9	99.9	860.39	861.53
18	[<i>p</i> NO ₂ Phe ²⁴]26RFa _(20–26)	LV-2236	19.0	99.9	860.39	861.46
19	[<i>p</i> NO ₂ Phe ²⁶]26RFa _(20–26)	LV-2194	18.9	99.9	860.39	861.56
20	[Phg ²²]26RFa _(20–26) <i>dia</i> 2	LV-2053	24.2	97.8	801.39	802.40
21	[Phg ²⁴]26RFa _(20–26) <i>dia</i> 1	LV-2054	21.1	99.9	801.39	802.40
22	[Phg ²⁴]26RFa _(20–26) <i>dia</i> 2	LV-2055	22.2	98.3	801.39	802.40
23	[Phg ²⁶]26RFa _(20–26) <i>dia</i> 1	LV-2056	21.0	99.9	801.39	802.70
24	[Phg ²⁶]26RFa _(20–26) <i>dia</i> 2	LV-2057	21.6	97.3	801.39	802.62
25	[NMePhe ²²]26RFa _(20–26)	LV-2066	18.9	99.9	829.42	830.53
26	[NMePhe ²⁴]26RFa _(20–26)	LV-2233	19.2	98.9	829.42	830.48
27	[NMePhe ²⁶]26RFa _(20–26)	LV-2242	18.8	99.9	829.42	830.48
28	[Tic ²²]26RFa _(20–26)	LV-2211	20.3	99.9	827.41	828.42
29	[Tic ²⁴]26RFa _(20–26)	LV-2205	17.7	99.9	827.41	828.46
30	[Tic ²⁶]26RFa _(20–26)	LV-2189	18.5	99.9	827.41	828.53
31	[NPhe ²²]26RFa _(20–26)	LV-2058	21.1	99.9	815.41	816.23
32	[NPhe ²⁴]26RFa _(20–26)	LV-2060	17.9	99.9	815.41	816.56
33	[NPhe ²⁶]26RFa _(20–26)	LV-2061	18.6	99.9	815.41	816.40
34	[AHPPA ²²]26RFa _(20–26)	LV-2062	17.8	99.9	859.43	860.30
35	[AHPPA ²⁴]26RFa _(20–26)	LV-2063	17.7	99.9	859.43	860.40
36	[AHPPA ²⁶]26RFa _(20–26)	LV-2064	18.1	99.9	859.43	860.55
37	[DTrp ²²]26RFa _(20–26)	LV-2237	18.2	99.9	854.42	855.56
38	[DTrp ²⁴]26RFa _(20–26)	LV-2070	17.7	99.9	854.42	855.53
39	[DTrp ²⁶]26RFa _(20–26)	LV-2188	18.2	99.9	854.42	855.39
40	[DTic ²²]26RFa _(20–26)	LV-2212	18.4	99.9	827.41	828.49
41	[DTic ²⁴]26RFa _(20–26)	LV-2215	18.2	99.9	827.41	828.36
42	[DTic ²⁶]26RFa _(20–26)	LV-2190	18.3	99.9	827.41	828.41
43	[Oic ²²]26RFa _(20–26)	LV-2067	18.6	99.9	819.44	820.56
44	[Oic ²⁴]26RFa _(20–26)	LV-2234	18.3	99.9	819.44	820.36
45	[Oic ²⁶]26RFa _(20–26)	LV-2241	18.1	99.9	819.44	820.45
46	[Cys ^{22,24}]26RFa _(20–26)	LV-2105	11.5	99.9	725.27	726.28
47	[Cys ^{22,26}]26RFa _(20–26)	LV-2107	6.7	99.9	725.27	726.37
48	[Cys ^{24,26}]26RFa _(20–26)	LV-2106	11.8	99.9	725.27	726.32

^a Retention time determined by analytical RP-HPLC. ^b Theoretical monoisotopic molecular weight. ^c *m/z* [MH]⁺ value assessed by MALDI-TOF-MS. AHPPA, (3*S*,4*S*)-4-amino-3-hydroxy-5-phenylpentanoic acid; 2Nal, 3-(2-naphtyl)-alanine; NMePhe, *N*-methyl-phenylalanine; NPhe, *N*-benzyl-glycine; Oic, octahydroindole-2-carboxylic acid; Pcp, (4-chloro)-phenylalanine; Phg, phenylglycine; *p*NO₂Phe, (4-nitro)-phenylalanine; *pt*BuPhe, (4-*ter*butyl)-phenylalanine; Thi, 3-(2-thienyl)-alanine; Tic, 1,2,3,4-tetrahydroisoquinoline-3-carboxylic acid. Diastereoisomers are numbered according to their elution order in RP-HPLC.

Table 2. Biological data for 26RFa_(20–26) analogs substituted in positions 22, 24 and 26.

	Peptide	Code	EC ₅₀		IC ₅₀		Imax (%) ^a
				(nM)		(nM)	
1	26RFa _(20–26)	LV-2021	1640	±	259	-	
2	[Thi ²²]26RFa _(20–26)	LV-2050	3160	±	1110	-	
3	[Thi ²⁴]26RFa _(20–26)	LV-2051	2530	±	1020	-	
4	[Thi ²⁶]26RFa _(20–26)	LV-2052	7227	±	96	-	
5	[2Nal ²²]26RFa _(20–26)	LV-2065	1150	±	170	-	
6	[2Nal ²⁴]26RFa _(20–26)	LV-2213	15,300	±	5400	-	
7	[2Nal ²⁶]26RFa _(20–26)	LV-2191	3790	±	1800	-	
8	[Trp ²²]26RFa _(20–26)	LV-2210	1980	±	880	-	
9	[Trp ²⁴]26RFa _(20–26)	LV-2204	2040	±	1600	-	
10	[Trp ²⁶]26RFa _(20–26)	LV-2187	5060	±	1300	-	
11	[<i>pt</i> BuPhe ²²]26RFa _(20–26)	LV-2068	>10,000		6220	±	2500
12	[<i>pt</i> BuPhe ²⁴]26RFa _(20–26)	LV-2235	>10,000			ND	
13	[<i>pt</i> BuPhe ²⁶]26RFa _(20–26)	LV-2238	1040	±	25 **	-	
14	[Pcp ²²]26RFa _(20–26)	LV-2069	5000	±	4500	-	
15	[Pcp ²⁴]26RFa _(20–26)	LV-2232	850	±	240 ^{NS}	-	
16	[Pcp ²⁶]26RFa _(20–26)	LV-2193	457	±	71 **	-	
17	[<i>p</i> NO ₂ Phe ²²]26RFa _(20–26)	LV-2214	2130	±	1100	-	
18	[<i>p</i> NO ₂ Phe ²⁴]26RFa _(20–26)	LV-2236	>10,000			ND	
19	[<i>p</i> NO ₂ Phe ²⁶]26RFa _(20–26)	LV-2194	491	±	33 **	-	
20	[Phg ²²]26RFa _(20–26) <i>dia</i> 1	LV-2053	5010	±	3600	-	
21	[Phg ²⁴]26RFa _(20–26) <i>dia</i> 1	LV-2054	>10,000			ND	
22	[Phg ²⁴]26RFa _(20–26) <i>dia</i> 2	LV-2055	>10,000			ND	
23	[Phg ²⁶]26RFa _(20–26) <i>dia</i> 1	LV-2056	>10,000			ND	
24	[Phg ²⁶]26RFa _(20–26) <i>dia</i> 2	LV-2057	>10,000			ND	
25	[NMePhe ²²]26RFa _(20–26)	LV-2066	15,100	±	4200	-	
26	[NMePhe ²⁴]26RFa _(20–26)	LV-2233	1360	±	750	-	
27	[NMePhe ²⁶]26RFa _(20–26)	LV-2242	>10,000			ND	
28	[Tic ²²]26RFa _(20–26)	LV-2211	327	±	170 *	-	
29	[Tic ²⁴]26RFa _(20–26)	LV-2205	>10,000			ND	
30	[Tic ²⁶]26RFa _(20–26)	LV-2189	7700	±	4400	-	
31	[NPhe ²²]26RFa _(20–26)	LV-2058	578	±	110 *	-	
32	[NPhe ²⁴]26RFa _(20–26)	LV-2060	>10,000			ND	
33	[NPhe ²⁶]26RFa _(20–26)	LV-2061	>10,000			ND	
34	[AHPPA ²²]26RFa _(20–26)	LV-2062	2850	±	380	-	
35	[AHPPA ²⁴]26RFa _(20–26)	LV-2063	>10,000			ND	
36	[AHPPA ²⁶]26RFa _(20–26)	LV-2064	>10,000			ND	
37	[DTrp ²²]26RFa _(20–26)	LV-2237	6160	±	2400	-	
38	[DTrp ²⁴]26RFa _(20–26)	LV-2070	>10,000			ND	
39	[DTrp ²⁶]26RFa _(20–26)	LV-2188	>10,000			>10,000	46
40	[DTic ²²]26RFa _(20–26)	LV-2212	4990	±	2100	-	
41	[DTic ²⁴]26RFa _(20–26)	LV-2215	6200	±	2600	-	
42	[DTic ²⁶]26RFa _(20–26)	LV-2190	>10,000			ND	
43	[Oic ²²]26RFa _(20–26)	LV-2067	>10,000			ND	
44	[Oic ²⁴]26RFa _(20–26)	LV-2234	>10,000			ND	
45	[Oic ²⁶]26RFa _(20–26)	LV-2241	>10,000			ND	
46	[Cys ^{22,24}]26RFa _(20–26)	LV-2105	>10,000			ND	
47	[Cys ^{22,26}]26RFa _(20–26)	LV-2107	>10,000			ND	
48	[Cys ^{24,26}]26RFa _(20–26)	LV-2106	>10,000			ND	

^a Inhibition at a maximal concentration of 10⁻⁵ M. Data are mean ± SEM of at least three independent experiments performed in triplicate. AHPPA, (3*S*,4*S*)-4-amino-3-hydroxy-5-phenylpentanoic acid; 2Nal, 3-(2-naphtyl)-alanine; NMePhe, *N*-methyl-phenylalanine; NPhe, *N*-benzyl-glycine; Oic, octahydroindole-2-carboxylic acid; Pcp, (4-chloro)-phenylalanine; Phg, phenylglycine; *p*NO₂Phe, (4-nitro)-phenylalanine; *pt*BuPhe, (4-*ter*butyl)-phenylalanine; Thi, 3-(2-thienyl)-alanine; Tic, 1,2,3,4-tetrahydroisoquinoline-3-carboxylic acid. Diastereoisomers are numbered according to their elution order in RP-HPLC. ND, not detectable. NS, not significant. * *p* < 0.05, ** *p* < 0.01 vs. control 26RFa_(20–26) (LV-2021, 1) as assessed by Mann and Whitney test.

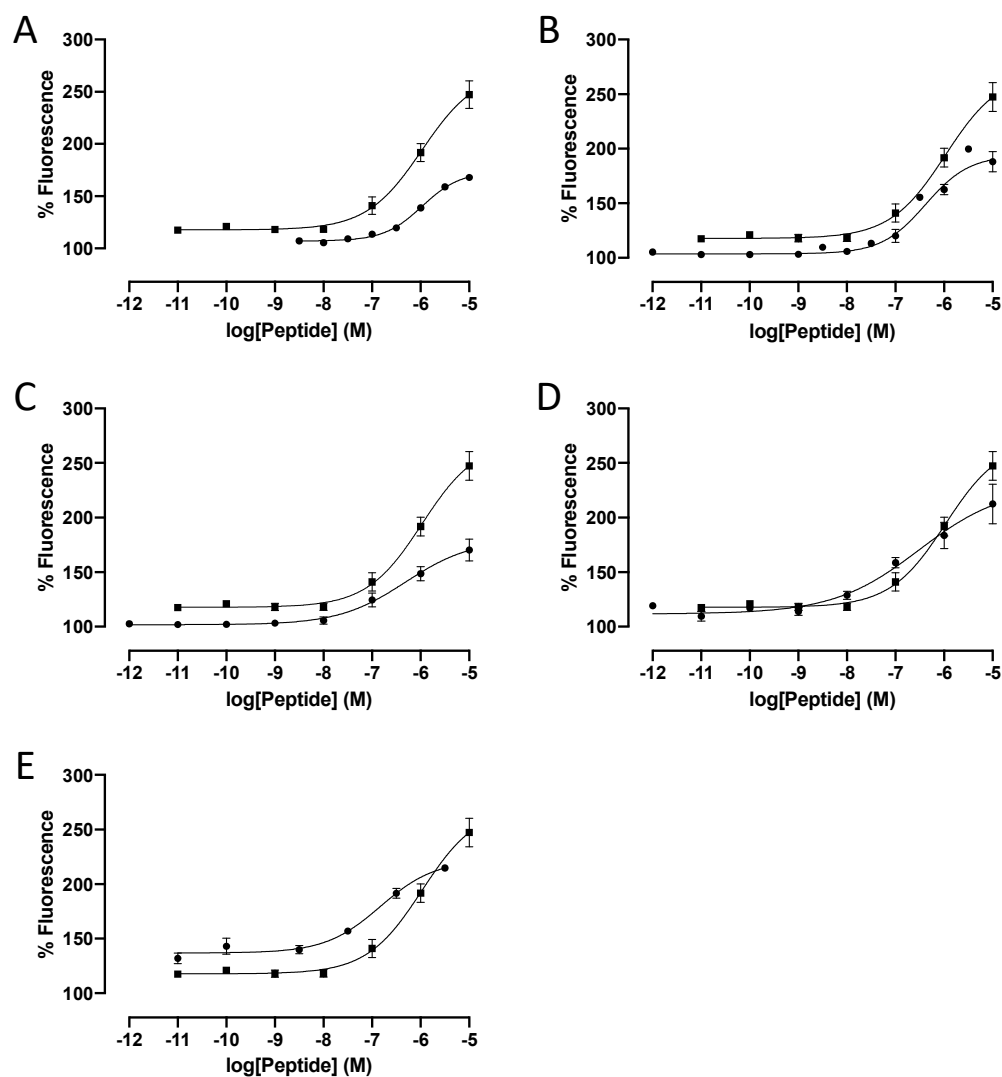


Figure 3. Effect of graded concentrations of Phe-modified 26RFa_(20–26) analogs on basal [Ca²⁺]_i mobilization in G_{α16}-*h*QRFPR-transfected CHO cells. Prototype dose–response curves of 26RFa_(20–26) (LV-2021, **1**, closed square, (A–E)) and its analogs (closed circles) [*pt*BuPhe²⁶]26RFa_(20–26) (LV-2238, **13**, (A)), [Pcp²⁶]26RFa_(20–26) (LV-2193, **16**, (B)), [*p*NO₂Phe²⁶]26RFa_(20–26) (LV-2194, **19**, (C)), [Tic²²]26RFa_(20–26) (LV-2211, **28**, (D)) and [Nphe²²]26RFa_(20–26) (LV-2058, **31**, (E)). Data are mean ± SEM of triplicate. The EC₅₀ calculated from these representative dose–response curves were 1069 nM for **1** (LV-2021), 1076 nM for **13** (LV-2238), 416 nM for **16** (LV-2193), 489 nM for **19** (LV-2194), 305 nM for **28** (LV-2211) and 149 nM for **31** (LV-2058).

The heptapeptide 26RFa_(20–26) does not encompass any secondary amide bonds within its backbone. Thus, nine analogs with *N*-methyl-phenylalanine (*N*MePhe), 1,2,3,4-tetrahydroisoquinoline-3-carboxylic acid (Tic) or *N*-benzyl-glycine (*N*Phe) were synthesized. These modifications were aimed at analyzing the significance of H-bond contributions of the amide NHs. Alkylation of these NHs without loss of agonistic activity would facilitate further analog design. *N*-methylation of Phe²² (LV-2066, **25**) and Phe²⁶ (LV-2242, **27**) nullified the activity of the parent compound (EC₅₀ > 10 μM, Table 2) revealing the critical role of the corresponding NHs in forming an H-bond with the *h*QRFPR pocket residues or another residue of the peptide, whereas *N*-methylation of Phe²⁴ (LV-2233, **26**) did not impair the whole activity of LV-2021 (**1**). The corresponding Tic-containing analogs (**28–30**) did not totally confirm these data since [Tic²⁴]26RFa_(20–26) (LV-2205, **29**) and [Tic²⁶]26RFa_(20–26) (LV-2189, **30**) were devoid of effect while [Tic²²]26RFa_(20–26) (LV-2211, **28**) was 5-fold more potent than 26RFa_(20–26) (LV-2021, **1**) (Figure 3D). It is thus also

plausible that the structural constraint induced by the Tic²² residue may keep the side chain in a favorable conformation for receptor activation, which was less accessible by free rotation in the native Phe side chain. The NPhe-peptoid analogs (31–33) behaved like the Tic-containing counterparts, and [NPhe²²]26RFa_(20–26) (LV-2058, 31) was almost as potent as LV-2211 (Table 2, Figure 3E). At this stage, conclusions are compromised since the local conformational rigidity to peptide backbone via pipecolinic acid bridge [46] and the shift of side chain functionality from the α -carbon to the NH offering flexibility to peptoid led to similar results. However, we can speculate that the Phe²² residue, which does not dive deeply into the binding pocket, accommodated rather well with backbone modifications at the odds to Phe²⁴ and Phe²⁶ which are strongly embedded in the orthosteric binding site [45]. An increase in H-bond capacity and flexibility by the introduction of (3S,4S)-4-amino-3-hydroxy-5-phenylpentanoic acid (AHPPA), a marine *Cyanobacterium symploca* peptide naturally occurring γ -amino acid [47] (34–36) had no positive effect on the potency of the parent heptapeptide (Table 2).

We have previously reported that stereoinversion to D-Phe in [DPhe²²]26RFa_(20–26), [DPhe²⁴]26RFa_(20–26) and [DPhe²⁶]26RFa_(20–26) results in a complete loss of the [Ca²⁺]_i response [36]. Similarly, successive D-Trp and D-Tic incorporation within the 26RFa_(20–26) sequence in the same positions generated weak (LV-2237, 37; LV-2212, 40; LV-2215, 41) or inactive (LV-2070, 38; LV-2188, 39; LV-2190, 42) agonists (Table 2), confirming that not only side chain functionality but also its correct orientation play a critical role in the activity of the peptide.

Systematic replacement of the three Phe units with the constrained aliphatic residue octahydroindole-2-carboxylic acid (Oic) yielded LV-2067 (43), LV-2234 (44) and LV-2241 (45) that were totally devoid of Ca²⁺-mobilizing activity (Table 2). The Oic moiety might induce a turn, like the prolyl residue [48], that would destabilize at this point the correct folding of the peptide backbone in the hQRFPR binding pocket. Furthermore, these results also confirm the importance of aromaticity in positions 22, 24 and 26 of 26RFa_(20–26) in the receptor activation process.

In methanol, 26RFa adopts a well-defined conformation consisting of a N-terminal amphipathic α -helical structure (Pro⁴–Arg¹⁷), preceding a C-terminal disordered region [49]. Interestingly, it has been shown that two Phe residues in an *i, i+4* arrangement (Phe²² and Phe²⁶ of 26RFa and 26RFa_(20–26)) enthalpically stabilize an α -helix [50]. To assess such a conformation of the C-terminal extremity of the peptide inside the hQRFPR binding pocket during the recognition process, we prepared cyclic disulfide-bridged 26RFa_(20–26) analogs (Table 1, 46–48) as already reported for the pentapeptide Met-enkephalin [51]. The activity profiles of [Cys^{22,26}]26RFa_(20–26) (LV-2107, 47), [Cys^{22,24}]26RFa_(20–26) (LV-2105, 46) and [Cys^{24,26}]26RFa_(20–26) (LV-2106, 48) did not confirm that the Phe residues of 26RFa_(20–26) (LV-2021, 1) participate in the bioactive conformation of the peptide or that some mandatory features are absent of these analogs (Table 2).

Compounds inactive as agonists were evaluated as possible antagonists of 26RFa-evoked calcium increase in cultured G _{α 16}-hQRFPR-transfected CHO cells. None of the members of this series were able to reverse the stimulatory effect of 10^{−7} M 26RFa on [Ca²⁺]_i, except LV-2068 (11) and LV-2188 (39) which antagonized 45–46% of the agonistic response with, respectively, modest and very low IC₅₀ (Table 2, Figure 4).

To summarize, the three phenylalanine units exhibit differential contributions to the biological activity of 26RFa_(20–26). The Phe²² residue appears to be the most permissive as it tolerated *N*-substitution like in [Tic²²]26RFa_(20–26) (LV-2211, 28) which was 5-folds more potent than the lead peptide. Conversely, most modifications of Phe²⁴ and Phe²⁶ did not improve the activity with the exception of para substituents of lesser size than that of a *tert*butyl group. Indeed, [Pcp²⁴]26RFa_(20–26) (LV-2232, 15), [Pcp²⁶]26RFa_(20–26) (LV-2193, 16) and [pNO₂Phe²⁶]26RFa_(20–26) (LV-2194, 19) were 2-, 3.5- and 3.3-fold more potent than 26RFa_(20–26) (LV-2021, 1). Although the amide NH of Phe²⁴ residue was probably not involved in H-bond, our results suggest that some flexibility of the peptide backbone is required at this point. Noteworthy, not only the H-bond capacity, but other features were

also impacted by these modifications such as the side chain presentation geometry, amide cis/trans isomerization equilibrium, and/or β -sheet potential of the analog with a wide range of steric, electronic and hydrophobic characteristics.

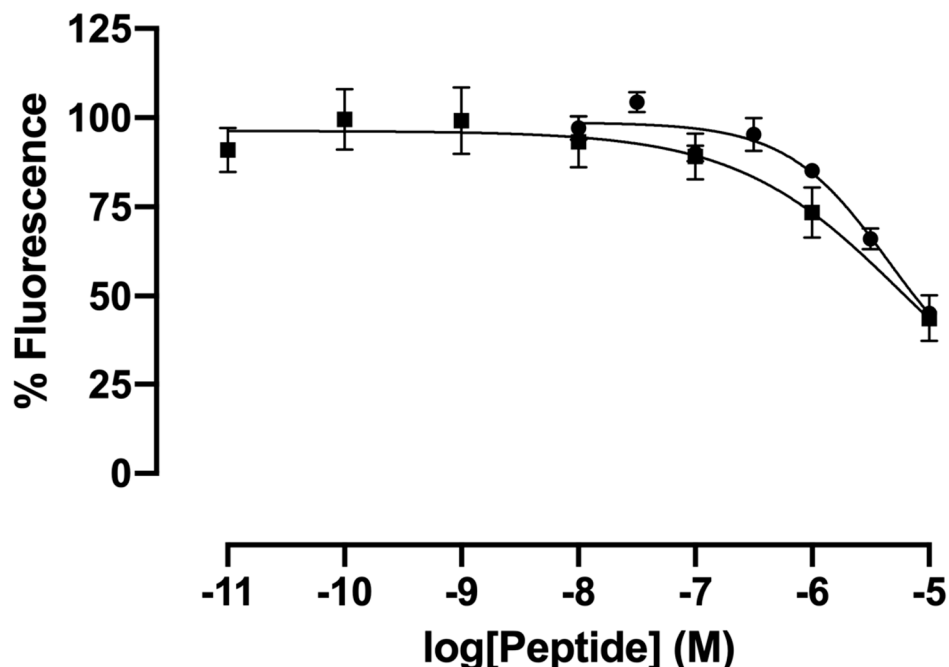


Figure 4. Effect of graded concentrations of Phe-modified 26RFa_(20–26) analogs on 26RFa-evoked $[Ca^{2+}]_i$ mobilization in $G_{\alpha 16}$ -*h*QRFPR-transfected CHO cells. Prototype dose-inhibition curves of [*pt*BuPhe²²]26RFa_(20–26) (LV-2068, **11**, closed circles) and [DTrp²⁶]26RFa_(20–26) (LV-2188, **39**, closed squares) on 10^{-7} M 26RFa-evoked response. Data are mean \pm SEM of triplicate. The IC₅₀ value calculated from these representative dose–inhibition curves were 4495 nM for **11** (LV-2068) and 5841 nM for **39** (LV-2188).

2.2. Impact of Concomitant Modifications of Gly²⁰, Gly²¹ and Phe²² Residues

The variety of conformations characterized in enkephalins [52] and other short peptide models containing contiguous Gly units [53] reveals an important heterogeneity in 3D structures of the Gly-Gly segment influenced by both neighboring residues and environment. In the homology model of *h*QRFPR, the Gly-Gly motif of 26RFa_(19–26) seems to adopt an extended conformation [45] generally observed in β -strands that form part of β -sheets. We have previously investigated the local requirement of the N-terminal dipeptide extremity of 26RFa_(20–26) and one of the most interesting results has been achieved by introducing a 4-carboxymethylpiperazine (Cmpi) unit in place of the native Gly-Gly pair which leads to the 5-fold more potent analog [Cmpi²¹]26RFa_(21–26) (LV-2043) than the reference heptapeptide [37]. Herein, to probe the space around this peptidomimetic moiety, we have introduced 2-piperazino-2-aryl-acetic acid racemate derivatives (Figure 5) in place of the first three 26RFa_(20–26) residues (Table 3) and evaluated the in vitro activity of each diastereoisomer (Table 4). In this series, analogs LV-2102 (**52**) and LV-2175 (**55**) containing 2-piperazino-2-[(4-fluoro)phenyl]acetic acid (Cmpi(4-FPhg)) and 2-piperazino-2-[(2-fluoro)phenyl]acetic acid (Cmpi(2-FPhg)) respectively, demonstrated similar $[Ca^{2+}]_i$ -mobilizing activity in *h*QRFPR-transfected cells compared to the lead peptide, while other derivatives exhibited slightly (LV-2101, **51**; LV-2103, **53**; LV-2104 **54**; LV-2183, **63**) or detrimentally lower potency (Table 4). Altogether, these results suggest that incorporation of an aryl substituent on the methylene of the Cmpi building block with the concomitant deletion of the Phe²² residues do neither improve the ability of [Cmpi²¹]26RFa_(21–26) to activate *h*QRFPR nor reverse the 26RFa-evoked effect.

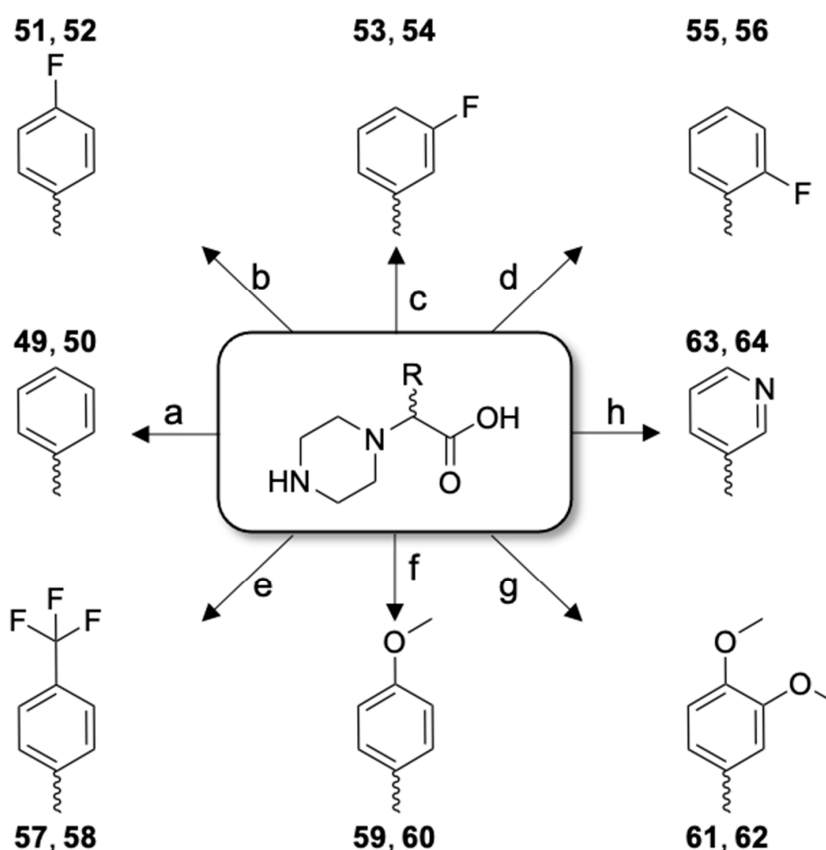


Figure 5. 2-Piperazino-2-aryl-acetic acid derivatives used in place of the H-Gly-Gly-Phe- sequence and incorporated in 49–64. These peptidomimetic moieties were used as racemate.

Table 3. Chemical data for 26RFa_(22–26) analogs.

Peptide Derivative	Code	HPLC		MS		
		Rt (min) ^a	Purity (%)	Calcd ^b	Obsd ^c	
1	26RFa _(20–26)	LV-2021	18.0	99.9	815.41	816.53
49	[Cmpi(Phg) ²²]26RFa _(22–26) dia 1	LV-2099	12.8	99.9	756.41	757.46
50	[Cmpi(Phg) ²²]26RFa _(22–26) dia 2	LV-2100	12.9	99.9	756.41	757.46
51	[Cmpi(4-FPhg) ²²]26RFa _(22–26) dia 1	LV-2101	15.3	99.9	774.40	775.37
52	[Cmpi(4-FPhg) ²²]26RFa _(22–26) dia 2	LV-2102	15.7	99.9	774.40	775.39
53	[Cmpi(3-FPhg) ²²]26RFa _(22–26) dia 1	LV-2103	15.3	99.9	774.40	775.42
54	[Cmpi(3-FPhg) ²²]26RFa _(22–26) dia 2	LV-2104	15.8	99.9	774.40	775.41
55	[Cmpi(2-FPhg) ²²]26RFa _(22–26) dia 1	LV-2175	13.9	98.4	774.40	775.47
56	[Cmpi(2-FPhg) ²²]26RFa _(22–26) dia 2	LV-2176	14.7	99.9	774.40	775.53
57	[Cmpi(4-TfmPhg) ²²]26RFa _(22–26) dia 1	LV-2177	25.3	99.9	824.39	825.47
58	[Cmpi(4-TfmPhg) ²²]26RFa _(22–26) dia 2	LV-2178	26.2	99.9	824.39	825.39
59	[Cmpi(4-MeOPhg) ²²]26RFa _(22–26) dia 1	LV-2179	13.2	99.9	786.42	787.47
60	[Cmpi(4-MeOPhg) ²²]26RFa _(22–26) dia 2	LV-2180	13.4	99.9	786.42	787.41
61	[Cmpi(3,4-diMeOPhg) ²²]26RFa _(22–26) dia 1	LV-2181	10.9	99.9	816.43	817.37
62	[Cmpi(3,4-diMeOPhg) ²²]26RFa _(22–26) dia 2	LV-2182	11.5	99.9	816.43	817.49
63	[Cmpi(3-Pyg) ²²]26RFa _(22–26) dia 1	LV-2183	19.5	99.9	757.40	758.40
64	[Cmpi(3-Pyg) ²²]26RFa _(22–26) dia 2	LV-2184	20.3	99.9	757.40	758.31

^a Retention time determined by analytical RP-HPLC. ^b Theoretical monoisotopic molecular weight. ^c m/z [MH]⁺ value assessed by MALDI-TOF-MS. Cmpi(Phg), 2-piperazino-2-phenylacetic acid; Cmpi(2-FPhg), 2-piperazino-2-[(2-fluoro)phenyl]acetic acid; Cmpi(3-FPhg), 2-piperazino-2-[(3-fluoro)phenyl]acetic acid; Cmpi(4-FPhg), 2-piperazino-2-[(4-fluoro)phenyl]acetic acid; Cmpi(4-TfmPhg), 2-piperazino-2-[(4-trifluoromethyl)phenyl]acetic acid; Cmpi(4-MeOPhg), 2-piperazino-2-[(4-methoxy)phenyl]acetic acid; Cmpi(3,4-diMeOPhg), 2-piperazino-2-[(3,4-dimethoxy)phenyl]acetic acid; Cmpi(3-Pyg), 2-piperazino-2-(3-pyridyl)acetic acid. Diastereoisomers are numbered according to their elution order in RP-HPLC.

Table 4. Biological data for 26RFa_(22–26) analogs.

	Peptide Derivative	Code	EC ₅₀		IC ₅₀	
				(nM)	(nM)	
1	26RFa _(20–26)	LV-2021	1640	±	259	-
49	[Cmpi(Phg) ²²]26RFa _(22–26) dia 1	LV-2099	>10,000			ND
50	[Cmpi(Phg) ²²]26RFa _(22–26) dia 2	LV-2100	>10,000			ND
51	[Cmpi(4-FPhg) ²²]26RFa _(22–26) dia 1	LV-2101	4050	±	1200	-
52	[Cmpi(4-FPhg) ²²]26RFa _(22–26) dia 2	LV-2102	1660	±	788	-
53	[Cmpi(3-FPhg) ²²]26RFa _(22–26) dia 1	LV-2103	3560	±	440	-
54	[Cmpi(3-FPhg) ²²]26RFa _(22–26) dia 2	LV-2104	2710	±	1000	-
55	[Cmpi(2-FPhg) ²²]26RFa _(22–26) dia 1	LV-2175	2480	±	1113	-
56	[Cmpi(2-FPhg) ²²]26RFa _(22–26) dia 2	LV-2176	>10,000			ND
57	[Cmpi(4-TfmPhg) ²²]26RFa _(22–26) dia 1	LV-2177	>10,000			ND
58	[Cmpi(4-TfmPhg) ²²]26RFa _(22–26) dia 2	LV-2178	>10,000			ND
59	[Cmpi(4-MeOPh) ²²]26RFa _(22–26) dia 1	LV-2179	>10,000			ND
60	[Cmpi(4-MeOPh) ²²]26RFa _(22–26) dia 2	LV-2180	>10,000			ND
61	[Cmpi(3,4-diMeOPh) ²²]26RFa _(22–26) dia 1	LV-2181	>10,000			ND
62	[Cmpi(3,4-diMeOPh) ²²]26RFa _(22–26) dia 2	LV-2182	>10,000			ND
63	[Cmpi(3-Pyg) ²²]26RFa _(22–26) dia 1	LV-2183	4990	±	2800	-
64	[Cmpi(3-Pyg) ²²]26RFa _(22–26) dia 2	LV-2184	>10,000			ND

Data are mean ± SEM of at least three independent experiments performed in triplicate. Cmpi(Phg), 2-piperazino-2-phenylacetic acid; Cmpi(2-FPhg), 2-piperazino-2-[(2-fluoro)phenyl]acetic acid; Cmpi(3-FPhg), 2-piperazino-2-[(3-fluoro)phenyl]acetic acid; Cmpi(4-FPhg), 2-piperazino-2-[(4-fluoro)phenyl]acetic acid; Cmpi(4-TfmPhg), 2-piperazino-2-[(4-trifluoromethyl)phenyl]acetic acid; Cmpi(4-MeOPh), 2-piperazino-2-[(4-methoxy)phenyl]acetic acid; Cmpi(3,4-diMeOPh), 2-piperazino-2-[(3,4-dimethoxy)phenyl]acetic acid; Cmpi(3-Pyg), 2-piperazino-2-(3-pyridyl)acetic acid. Diastereoisomers are numbered according to their elution order in RP-HPLC. ND, not detectable.

3. Materials and Methods

3.1. Reagents

All Fmoc-amino acid residues and building blocks and O-benzotriazol-1-yl-*N,N,N',N'*-tetramethyluronium hexafluorophosphate (HBTU) were purchased from Christof Senn Laboratories (Dielsdorf, Switzerland) or PolyPeptide (Strasbourg, France). Rink amide 4-methylbenzhydrylamine (MBHA) resin was from Novabiochem (Darmstadt, Germany) and *N*-methylpyrrolidone (NMP), dimethylformamide (DMF) and dichloromethane (DCM) were from Biosolve (Dieuze, France). *N,N*-Diisopropylethylamine (DIEA), piperidine, trifluoroacetic acid (TFA), triisopropylsilane (TIS), *tert*-butylmethylether (TBME) were supplied from Sigma-Aldrich (Saint-Quentin-Fallavier, France). Acetonitrile was from Fisher Scientific (Illkirch, France) and α -cyano-4-hydroxycinnamic acid (CHCA) matrix from LaserBioLabs (Valbonne, France).

3.2. Peptide Synthesis and Purification

All peptides and derivatives were synthesized by the solid phase methodology on Rink amide MBHA resin using a Liberty microwave-assisted automated peptide synthesizer (CEM, Saclay, France) and the standard manufacturer's procedures at 0.1 mmol scale as previously described [54]. All Fmoc-amino acids and building blocks (0.5 mmol, 5 equiv) were coupled by in situ activation with HBTU (0.5 mmol, 5 equiv) and DIEA (1 mmol, 10 equiv). Peptides and derivatives were deprotected and cleaved from the resin by adding a TFA/TIS/H₂O (99.5/0.25/0.25) mixture for 120 min at room temperature. After filtration, crude peptides were precipitated by addition of TBME, centrifuged and recovered by elimination of the supernatant (3 folds). Peptides and derivatives were purified by reversed-phase HPLC (RP-HPLC) on a 2.2 × 25 cm Vydac 218TP1022 C₁₈ column (Grace, Epneron, France) using a linear gradient (10–40%, 10–50%, 10–60%, 20–40%, 20–50% or 20–60% over 45 min) of acetonitrile/TFA (99.9/0.1) at a flow rate of 10 mL/min. The purified peptides were then characterized by MALDI-TOF mass spectrometry on a UltrafleXtreme (Bruker, Strasbourg, France) using CHCA as a matrix. Analytical RP-HPLC, performed on a 0.46 × 25 cm Vydac 218TP54 C₁₈ column (Grace), showed that the purity of all compounds was >97.3%.

3.3. Cell Culture

Stably transfected *hQRFPR* CHO cells were obtained as previously described [36–38]. The cells were maintained in F-12 nutrient mixture (Ham-F12) medium supplemented with 10% fetal bovine serum, 2 mM glutamine, and penicillin-streptomycin. Expression of $G_{\alpha 16}$ cells was maintained using selection antibiotic hygromycin B (200 $\mu\text{g}/\text{mL}$) and that of *hQRFPR* using geneticin G418 (500 $\mu\text{g}/\text{mL}$) (Life Technologies, Villebon-Sur-Yvette, France) in a humidified 5% CO_2 atmosphere at 37 °C.

3.4. Calcium Mobilization Assays

Changes in intracellular Ca^{2+} concentrations induced by 26RFa_(20–26) analogs in CHO- $G_{\alpha 16}$ -*hQRFPR*-transfected cells were measured on a benchtop scanning fluorometer Flexstation III (Molecular Devices, Sunnyvale, CA, USA) as previously described [36–38,55,56]. Briefly, 96-well assay black plates with clear bottoms (Corning international, Avon, France) were seeded at a density of 40,000 cells/well 24 h prior to assay. For profiling agonistic experiments, cells were loaded with 2 μM Fluo-4 acetoxymethyl ester (AM) (Invitrogen) for 1 h in the presence of 0.01% pluronic acid, washed thrice, and incubated for 30 min with standard HBSS containing 2.5 mM probenecid and 5 mM HEPES. Compounds to be tested were added at final concentrations ranging from 10^{-11} to 10^{-5} M in HBSS, and the fluorescence intensity was measured during 3 min. To evaluate the antagonistic potency of the test compounds, cells were incubated with each compound over 15 min after Fluo-4 AM loading. Then, during fluorescence recording, a pulse of 26RFa was administered at a final concentration of 10^{-7} M. After subtraction of the mean fluorescence background, the baseline was normalized to 100%. Fluorescence peak values were determined for each concentration of compound.

3.5. Statistical Analysis

Calcium experiments were performed in triplicate, and data, expressed as mean \pm SEM of at least three distinct experiments, were analyzed with the Prism 8.0 software (Graphpad Software, San Diego, CA, USA). EC_{50} and the IC_{50} values were determined from concentration–response curves using a sigmoidal dose–response fit with variable slope from at least three independent determinations. Differences between 26RFa_(20–26) and analog activities were analyzed by the Mann–Whitney test. p values < 0.05 were considered significant.

3.6. Nomenclature of Targets and Ligands

All targets and ligands used throughout this manuscript conform with the guidelines outlined by the International Union of Basic and Clinical Pharmacology and British Pharmacological Society (IUPHAR/BPS) Guide to Pharmacology [5,57].

4. Conclusions

The C-terminal extremity of 26RFa was previously identified as a pivotal region to modulate its signaling at *hQRFPR* [36]. In this work, the Phe²², Phe²⁴ and Phe²⁶ residues of 26RFa_(20–26) were modified using series of point substitutions with natural, side chain-constrained, side chain-modified residues and peptidomimetic building blocks. Subtle chemical modifications in the sequence led to significant improvement in compound potency to activate *hQRFPR*. As such, a single modification of Phe²² with the steric restricted Tic residue decreased the EC_{50} value from 1640 ± 259 to 327 ± 170 nM, providing the most efficient modification at this sequence position. Anchored substituents in the para position of each Phe unit were the most versatile investigated modification. Thereby, the introduction of a para-chloro-phenylalanine in place of the native Phe²⁴ moiety emerged as a favorable replacement. This finding follows the same trend observed in [Pcp²⁶]26RFa_(20–26), highlighting a limited room to accommodate aromatic residues around the Phe aryl group. Although combination of multiple point-effective modifications does not necessarily translate into an additive or synergic effect, we have explored each position of 26RFa_(20–26) for

complete optimization of its sequence. Future challenges will be to convert several of these point modifications to low molecular weight 26RFa analogs for metabolic disorder, obesity or diabetes therapies. We are confident that, by utilizing subtle amendments, we can design 26RFa_(20–26)-based compounds with nanomolar potency, functional selectivity and in vivo bioavailability.

Author Contributions: B.L. contributed to compound syntheses, acquisition of data, data analysis/interpretation, drafting of the manuscript. K.A., C.N., O.L.M. and C.D. participated in acquisition of data and their analysis/interpretation. J.A.B., J.C., D.V., G.P. and M.P. provided valuable editorial comments and relevant bibliographic references. H.V. and N.C. contributed to critical revision of the manuscript. J.L. conceived and designed the experiments with B.L., K.A. and C.N., contributed to data analysis/interpretation, drafting of the manuscript and approval of the article. All authors have read and agreed to the published version of the manuscript.

Funding: This work was supported by INSERM, the University of Normandy Rouen, the Region Normandy and the European Union. Europe gets involved in Normandy, with European Regional Development Fund (ERDF).

Institutional Review Board Statement: Not applicable.

Informed Consent Statement: Not applicable.

Data Availability Statement: All data are generated during this study.

Conflicts of Interest: The authors declare no competing financial interest.

Sample Availability: Samples of the compounds 1–64 are available from the authors.

Abbreviations

AHPPA: (3S,4S)-4-amino-3-hydroxy-5-phenylpentanoic acid; $[Ca^{2+}]_i$, intracellular calcium concentration; Cmpi, 4-carboxymethylpiperazine; Cmpi(2-FPhg), 2-piperazino-2-[(2-fluoro)phenyl]acetic acid; Cmpi(4-FPhg), 2-piperazino-2-[(4-fluoro)phenyl]acetic acid; hQRFPR, human QRFPR receptor; 2-Nal, 3-(2-naphthyl)-alanine; NMePhe, N-methyl-phenylalanine; NPhe, N-benzyl-glycine; Thi, 3-(2-thienyl)-alanine; Oic, octahydroindole-2-carboxylic acid; Phg, phenylglycine; Tic, 1,2,3,4-tetrahydroisoquinoline-3-carboxylic acid.

References

1. Chartrel, N.; Dujardin, C.; Anouar, Y.; Leprince, J.; Decker, A.; Clerens, S.; Do-Régo, J.-C.; Vandessande, F.; Llorens-Cortes, C.; Costentin, J.; et al. Identification of 26RFa, a hypothalamic neuropeptide of the RFamide peptide family with orexigenic activity. *Proc. Natl. Acad. Sci. USA* **2003**, *100*, 15247–15252. [[CrossRef](#)]
2. Fukusumi, S.; Yoshida, H.; Fujii, R.; Maruyama, M.; Komatsu, H.; Habata, Y.; Shintani, Y.; Hinuma, S.; Fujino, M. A new peptidic ligand and its receptor regulating adrenal function in rats. *J. Biol. Chem.* **2003**, *278*, 46387–46395. [[CrossRef](#)]
3. Jiang, Y.; Luo, L.; Gustafson, E.L.; Yadav, D.; Laverty, M.; Murgolo, N.; Vassileva, G.; Zeng, M.; Laz, T.M.; Behan, J.; et al. Identification and characterization of a novel RF-amide peptide ligand for orphan G-protein-coupled receptor SP9155. *J. Biol. Chem.* **2003**, *278*, 27652–27657. [[CrossRef](#)]
4. Chartrel, N.; Dujardin, C.; Leprince, J.; Desrues, L.; Tonon, M.-C.; Cellier, E.; Cosette, P.; Jouenne, T.; Simonnet, G.; Vaudry, H. Isolation, characterization and distribution of a novel neuropeptide, Rana RFamide (R-RFa), in the brain of the European green frog *Rana esculenta*. *J. Comp. Neurol.* **2002**, *448*, 111–127. [[CrossRef](#)]
5. Leprince, J.; Bagnol, D.; Bureau, R.; Fukusumi, S.; Granata, R.; Hinuma, S.; Larhammar, D.; Primeaux, S.; Sopkova-de Oliveira Santos, J.; Tsutsui, K.; et al. The Arg-Phe-amide peptide 26RFa/glutamine RF-amide peptide and its receptor. *IUPHAR Review* **2017**, *24*, 3573–3607. [[CrossRef](#)] [[PubMed](#)]
6. Ukena, K.; Tachibana, T.; Iwakoshi-Ukena, E.; Saito, Y.; Minakata, H.; Kawaguchi, R.; Osugi, T.; Tobari, Y.; Leprince, J.; Vaudry, H.; et al. Identification, localization, and function of a novel avian hypothalamic neuropeptide, 26RFa, and its cognate receptor, G protein-coupled receptor-103. *Endocrinology* **2010**, *151*, 2255–2264. [[CrossRef](#)] [[PubMed](#)]
7. Tobari, Y.; Iijima, N.; Tsunekawa, K.; Osugi, T.; Haraguchi, S.; Ubuka, T.; Ukena, K.; Okanoya, K.; Tsutsui, K.; Ozawa, H. Identification, localisation and functional implication of 26RFa orthologue peptide in the brain of zebra finch (*Taeniopygia guttata*). *J. Neuroendocrinol.* **2011**, *23*, 791–803. [[CrossRef](#)]

8. Takayasu, S.; Sakurai, T.; Iwasaki, S.; Teranishi, H.; Yamanaka, A.; Williams, S.C.; Iguchi, H.; Kawasaki, Y.I.; Ikeda, Y.; Sakakibara, I.; et al. A neuropeptide ligand of the G protein-coupled receptor GPR103 regulates feeding, behavioral arousal, and blood pressure in mice. *Proc. Natl. Acad. Sci. USA* **2006**, *103*, 7438–7443. [[CrossRef](#)] [[PubMed](#)]
9. Bruzzone, F.; Lectez, B.; Tollemer, H.; Leprince, J.; Dujardin, C.; Rachidi, W.; Chatenet, D.; Baroncini, M.; Beauvillain, J.-C.; Vallarino, M.; et al. Anatomical distribution and biochemical characterization of the novel RFamide peptide 26RFa in the human hypothalamus and spinal cord. *J. Neurochem.* **2006**, *99*, 616–627. [[CrossRef](#)] [[PubMed](#)]
10. Kampe, J.; Wiedmer, P.; Pfluger, P.T.; Castaneda, T.R.; Burget, L.; Mondala, H.; Kerr, J.; Liaw, C.; Oldfield, B.J.; Tschöp, M.H.; et al. Effect of central administration of QRFP(26) peptide on energy balance and characterization of a second QRFP receptor in rat. *Brain Res.* **2006**, *1119*, 133–149. [[CrossRef](#)]
11. Lectez, B.; Jeandel, L.; El-Yamani, F.-Z.; Arthaud, S.; Alexandre, D.; Mardargent, A.; Jégou, S.; Mounien, L.; Bizet, P.; Magoul, R.; et al. The orexigenic activity of the hypothalamic neuropeptide 26RFa is mediated by the neuropeptide Y and proopiomelanocortin neurons of the arcuate nucleus. *Endocrinology* **2009**, *150*, 2342–2350. [[CrossRef](#)] [[PubMed](#)]
12. Do Rego, J.-C.; Leprince, J.; Chartrel, N.; Vaudry, H.; Costentin, J. Behavioral effects of 26RFamide and related peptides. *Peptides* **2006**, *27*, 2715–2721. [[CrossRef](#)] [[PubMed](#)]
13. Moriya, R.; Sano, H.; Umeda, T.; Ito, M.; Takahashi, Y.; Matsuda, M.; Ishihara, A.; Kanatani, A.; Iwaasa, H. RFamide peptide QRFP43 causes obesity with hyperphagia and reduced thermogenesis in mice. *Endocrinology* **2006**, *147*, 2916–2922. [[CrossRef](#)] [[PubMed](#)]
14. Primeaux, S.D.; Blackmon, C.; Barnes, M.J.; Braymer, H.D.; Bray, G.A. Central administration of the RFamide peptides, QRFP-26 and QRFP-43, increases high fat food intake in rats. *Peptides* **2008**, *29*, 1994–2000. [[CrossRef](#)]
15. Primeaux, S.D.; Barnes, M.J.; Braymer, H.D. Hypothalamic QRFP: Regulation of food intake and fat selection. *Horm. Metab. Res.* **2013**, *45*, 967–974. [[CrossRef](#)] [[PubMed](#)]
16. Zagorác, O.; Kovács, A.; László, K.; Ollmann, T.; Péczely, L.; Lénárd, L. Effects of direct QRFP-26 administration into the medial hypothalamic area on food intake in rats. *Brain Res. Bull.* **2015**, *118*, 58–64. [[CrossRef](#)] [[PubMed](#)]
17. Navarro, V.M.; Fernández-Fernández, R.; Nogueiras, R.; Vigo, E.; Tovar, S.; Chartrel, N.; Le Marec, O.; Leprince, J.; Aguilar, E.; Pinilla, L.; et al. Novel role of 26RFa, a hypothalamic RFamide orexigenic peptide, as putative regulator of the gonadotropic axis. *J. Physiol.* **2006**, *573*, 237–249. [[CrossRef](#)]
18. Patel, S.R.; Murphy, K.G.; Thompson, E.L.; Patterson, M.; Curtis, A.E.; Ghatei, M.A.; Bloom, S.R. Pyroglutamylated RFamide peptide 43 stimulates the hypothalamic-pituitary-gonadal axis via gonadotropin-releasing hormone in rats. *Endocrinology* **2008**, *149*, 4747–4754. [[CrossRef](#)]
19. Palotai, M.; Telegdy, G. Anxiolytic effect of the GPR103 receptor agonist peptide P550 (homolog of neuropeptide 26RFa) in mice. Involvement of neurotransmitters. *Peptides* **2016**, *82*, 20–25. [[CrossRef](#)] [[PubMed](#)]
20. Zagorác, O.; Ollmann, T.; Péczely, L.; László, K.; Kovács, A.; Berta, B.; Kállai, V.; Kertes, E.; Lénárd, L. QRFP administration into the medial hypothalamic nuclei improves memory in rats. *Brain Res.* **2020**, *1727*, 146563. [[CrossRef](#)]
21. Yamamoto, T.; Miyazaki, R.; Yamada, T. Intracerebroventricular administration of 26RFa produces an analgesic effect in the rat formalin test. *Peptides* **2009**, *30*, 1683–1688. [[CrossRef](#)] [[PubMed](#)]
22. Yamamoto, T.; Miyazaki, R.; Yamada, T.; Shinozaki, T. Anti-allodynic effects of intrathecally and intracerebroventricularly administered 26RFa, an intrinsic agonist for GRP103, in the rat partial sciatic nerve ligation model. *Peptides* **2011**, *32*, 1262–1269. [[CrossRef](#)] [[PubMed](#)]
23. Yoshida, K.; Nonaka, T.; Nakamura, S.; Araki, M.; Yamamoto, T. Microinjection of 26RFa, an endogenous ligand for the glutamine RF-amide peptide receptor (QRFP receptor), into the rostral ventromedial medulla (RVM), locus coeruleus (LC), and periaqueductal grey (PAG) produces an analgesic effect in rats. *Peptides* **2019**, *115*, 1–7. [[CrossRef](#)]
24. Gouardères, C.; Mazarguil, H.; Mollereau, C.; Chartrel, N.; Leprince, J.; Vaudry, H.; Zajac, J.-M. Functional differences between NPFF1 and NPFF2 receptor coupling: High intrinsic activities of RFamide-related peptides on stimulation of [³⁵S]GTPγS binding. *Neuropharmacology* **2007**, *52*, 376–386. [[CrossRef](#)]
25. Chartrel, N.; Alonzeau, J.; Alexandre, D.; Jeandel, L.; Alvear-Perez, R.; Leprince, J.; Boutin, J.; Vaudry, H.; Anouar, Y.; Llorens-Cortes, C. The RFamide neuropeptide 26RFa and its role in the control of neuroendocrine functions. *Front. Neuroendocrinol.* **2011**, *32*, 387–397. [[CrossRef](#)]
26. Prévost, G.; Jeandel, L.; Arabo, A.; Coëffier, M.; El Ouahli, M.; Picot, M.; Alexandre, D.; Gobet, F.; Leprince, J.; Berrahmoune, H.; et al. Hypothalamic neuropeptide 26RFa acts as an incretin to regulate glucose homeostasis. *Diabetes* **2015**, *64*, 2805–2816. [[CrossRef](#)]
27. Prévost, G.; Arabo, A.; Le Solliec, M.-A.; Bons, J.; Picot, M.; Maucotel, J.; Berrahmoune, H.; El Mehdi, M.; Cherifi, S.; Benani, A.; et al. Neuropeptide 26RFa (QRFP) is a key regulator of glucose homeostasis and its activity is markedly altered in obese/hyperglycemic mice. *Am. J. Physiol. Endocrinol. Metab.* **2019**, *317*, E147–E157. [[CrossRef](#)]
28. Prévost, G.; Picot, M.; Le Solliec, M.-A.; Arabo, A.; Berrahmoune, H.; El Mehdi, M.; Cherifi, S.; Benani, A.; Nédélec, E.; Gobet, F.; et al. The neuropeptide 26RFa in the human gut and pancreas: Potential involvement in glucose homeostasis. *Endocr. Connect.* **2019**, *8*, 941–951. [[CrossRef](#)] [[PubMed](#)]
29. El-Mehdi, M.; Takhlidjt, S.; Khiar, F.; Prévost, G.; Do Rego, J.-L.; Do Rego, J.-C.; Benani, A.; Nédélec, E.; Godefroy, D.; Arabo, A.; et al. Glucose homeostasis is impaired in mice deficient in the neuropeptide 26RFa (QRFP). *BMJ Open Diabetes Res. Care* **2020**, *8*, e000942. [[CrossRef](#)] [[PubMed](#)]

30. Quillet, R.; Ayachi, S.; Bihel, F.; Elhabazi, K.; Ilien, B.; Simonin, F. RF-amide neuropeptides and their receptors in Mammals: Pharmacological properties, drug development and main physiological functions. *Pharmacol. Ther.* **2016**, *160*, 84–132. [[CrossRef](#)]
31. Mazarguil, H.; Gouardères, C.; Tafani, J.A.; Marcus, D.; Kotani, M.; Mollereau, C.; Roumy, M.; Zajac, J.M. Structure-activity relationships of neuropeptide FF: Role of C-terminal regions. *Peptides* **2001**, *22*, 1471–1478. [[CrossRef](#)]
32. Boyle, R.G.; Downham, R.; Ganguly, T.; Humphries, J.; Smith, J.; Travers, S. Structure-activity studies on prolactin-releasing peptide (PrRP). Analogues of PrRP-(19–31)-peptide. *J. Pept. Sci.* **2005**, *11*, 161–165. [[CrossRef](#)]
33. Orsini, M.J.; Klein, M.A.; Beavers, M.P.; Connolly, P.J.; Middleton, S.A.; Mayo, K.H. Metastin (KiSS-1) mimetics identified from peptide structure-activity relationship-derived pharmacophores and directed small molecule database screening. *J. Med. Chem.* **2007**, *50*, 462–471. [[CrossRef](#)] [[PubMed](#)]
34. Gicquel, S.; Mazarguil, H.; Desprat, C.; Allard, M.; Devillers, J.P.; Simonnet, G.; Zajac, J.M. Structure-activity study of neuropeptide FF: Contribution of N-terminal regions to affinity and activity. *J. Med. Chem.* **1994**, *37*, 3477–3481. [[CrossRef](#)]
35. Mazarguil, H.; Mollereau, C.; Czaplicki, G.; Zajac, J.M. Study of the N-terminal part of peptidic selective NPFF₂ agonists. *Peptides* **2012**, *37*, 157–160. [[CrossRef](#)] [[PubMed](#)]
36. Le Marec, O.; Neveu, C.; Lefranc, B.; Dubessy, C.; Boutin, J.A.; Do-Régo, J.-C.; Costentin, J.; Tonon, M.-C.; Tena-Sempere, M.; Vaudry, H.; et al. Structure-activity relationships of a series of analogues of the RFamide-related peptide 26RFa. *J. Med. Chem.* **2011**, *54*, 4806–4814. [[CrossRef](#)]
37. Neveu, C.; Lefranc, B.; Tasseau, O.; Do Rego, J.-C.; Bourmaud, A.; Chan, P.; Bauchat, P.; Le Marec, O.; Chuquet, J.; Guilhaudis, L.; et al. Rational design of a low molecular weight, stable, potent, and long-lasting GPR103 aza- β^3 -pseudopeptide agonist. *J. Med. Chem.* **2012**, *55*, 7516–7524. [[CrossRef](#)]
38. Alim, K.; Lefranc, B.; Sopkova-de Oliveira Santos, J.; Dubessy, C.; Picot, M.; Boutin, J.A.; Vaudry, H.; Chartrel, N.; Vaudry, D.; Chuquet, J.; et al. Design, synthesis, molecular dynamics simulation and functional evaluation of a novel series of 26RFa peptide analogues containing a mono- or polyalkyl guanidino arginine derivative. *J. Med. Chem.* **2018**, *61*, 10185–10197. [[CrossRef](#)]
39. Pierry, C.; Couve-Bonnaire, S.; Guilhaudis, L.; Neveu, C.; Marotte, A.; Lefranc, B.; Cahard, D.; Segalas-Milazzo, I.; Leprince, J.; Pannecoucke, X. Fluorinated pseudopeptide analogues of neuropeptide 26RFa: Synthesis, biological and structural studies. *ChemBioChem*. **2013**, *14*, 1620–1633. [[CrossRef](#)]
40. Rouméas, L.; Humbert, J.P.; Schneider, S.; Doebelin, C.; Bertin, I.; Schmitt, M.; Bourguignon, J.J.; Simonin, F.; Bihel, F. Effects of systematic N-terminus deletions and benzoylations of endogenous RF-amide peptides on NPFF1R, NPFF2R, GPR10, GPR54 and GPR103. *Peptides* **2015**, *71*, 156–161. [[CrossRef](#)] [[PubMed](#)]
41. Anjana, R.; Vaishnavi, M.K.; Sherlin, D.; Kumar, S.P.; Naveen, K.; Kanth, P.S.; Sekar, K. Aromatic-aromatic interactions in structures of proteins and protein-DNA complexes: A study based on orientation and distance. *Bioinformation* **2012**, *8*, 1220–1224. [[CrossRef](#)]
42. Makwana, K.M.; Mahalakshmi, R. Implications of aromatic-aromatic interactions: From protein structures to peptide models. *Protein Sci.* **2015**, *24*, 1920–1933. [[CrossRef](#)] [[PubMed](#)]
43. de Freitas, R.F.; Schapira, M. A systematic analysis of atomic protein-ligand interactions in the PDB. *MedChemComm* **2017**, *8*, 1970–1981. [[CrossRef](#)]
44. Meyer, E.A.; Castellano, R.K.; Diederich, F. Interactions with aromatic rings in chemical and biological recognition. *Angew. Chem. Int. Ed. Engl.* **2003**, *42*, 1210–1250. [[CrossRef](#)] [[PubMed](#)]
45. Neveu, C.; Dulin, F.; Lefranc, B.; Galas, L.; Calbrix, C.; Bureau, R.; Rault, S.; Chuquet, J.; Boutin, J.A.; Guilhaudis, L.; et al. Molecular basis of agonist docking in a human GPR103 homology model by site-directed mutagenesis and structure-activity relationship studies. *Br. J. Pharmacol.* **2014**, *171*, 4425–4439. [[CrossRef](#)]
46. Kotha, S.; Deodhar, D.; Khedkar, P. Diversity-oriented synthesis of medicinally important 1,2,3,4-tetrahydroisoquinoline-3-carboxylic acid (Tic) derivatives and higher analogs. *Org. Biomol. Chem.* **2014**, *12*, 9054–9091. [[CrossRef](#)]
47. Williams, P.G.; Yoshida, W.Y.; Moore, R.E.; Paul, V.J. The isolation and structure elucidation of Tasiamide B, a 4-amino-3-hydroxy-5-phenylpentanoic acid containing peptide from the marine *Cyanobacterium symploca* sp. *J. Nat. Prod.* **2003**, *66*, 1006–1009. [[CrossRef](#)] [[PubMed](#)]
48. Fauchère, J.L.; Thurieau, C. Evaluation of the stability of peptides and pseudopeptides as a tool in peptide drug design. *Adv. Drug Res.* **1992**, *23*, 127–158.
49. Thuau, R.; Guilhaudis, L.; Ségalas-Milazzo, I.; Chartrel, N.; Oulyadi, H.; Boivin, S.; Fournier, A.; Leprince, J.; Davoust, D.; Vaudry, H. Structural studies on 26RFa, a novel human RFamide-related peptide with orexigenic activity. *Peptides* **2005**, *26*, 779–789. [[CrossRef](#)]
50. Butterfield, S.M.; Patel, P.R.; Waters, M.L. Contribution of aromatic interactions to α -helix stability. *J. Am. Chem. Soc.* **2002**, *124*, 9751–9755. [[CrossRef](#)]
51. Mosberg, H.I.; Hurst, R.; Hruby, V.J.; Gee, K.; Yamamura, H.I.; Galligan, J.J.; Burks, T.F. Bis-penicillamine enkephalins possess highly improved specificity toward delta opioid receptors. *Proc. Natl. Acad. Sci. USA* **1983**, *80*, 5871–5874. [[CrossRef](#)]
52. Marcotte, I.; Separovic, F.; Auger, M.; Gagné, S.M. A multidimensional 1H NMR investigation of the conformation of methionine-enkephalin in fast-tumbling bicelles. *Biophys. J.* **2004**, *86*, 1587–1600. [[CrossRef](#)]
53. Datta, S.; Shamala, N.; Banerjee, A.; Balaram, P. Conformational variability of Gly-Gly segments in peptides: A comparison of the crystal structures of an acyclic pentapeptide and an octapeptide. *Biopolymers* **1997**, *41*, 331–336. [[CrossRef](#)]

54. Touchard, A.; Aili, S.R.; Téné, N.; Barassé, V.; Klopp, C.; Dejean, A.; Kini, R.M.; Mrinalini; Coquet, L.; Jouenne, T.; et al. Venom peptide repertoire of the European myrmicine ant *Manica rubida*: Identification of insecticidal toxins. *J. Proteome Res.* **2020**, *19*, 1800–1811. [[CrossRef](#)] [[PubMed](#)]
55. Dubessy, C.; Cartier, D.; Lectez, B.; Bucharles, C.; Chartrel, N.; Montero-Hadjadje, M.; Bizet, P.; Chatenet, D.; Tostivint, H.; Scalbert, E.; et al. Characterization of urotensin II, distribution of urotensin II, urotensin II-related peptide and UT receptor mRNAs in mouse: Evidence of urotensin II at the neuromuscular junction. *J. Neurochem.* **2008**, *17*, 361–374. [[CrossRef](#)] [[PubMed](#)]
56. Gutiérrez-Pascual, E.; Leprince, J.; Martínez-Fuentes, A.J.; Ségalas-Milazzo, I.; Pineda, R.; Roa, J.; Duran-Prado, M.; Guilhaudis, L.; Desperrois, E.; Lebreton, A.; et al. In vivo and in vitro structure-activity relationships and structural conformation of kisspeptin-10-related peptides. *Mol. Pharmacol.* **2009**, *76*, 58–67. [[CrossRef](#)]
57. Alexander, S.P.H.; Christopoulos, A.; Davenport, A.P.; Kelly, E.; Mathie, A.; Peters, J.A.; Veale, E.L.; Armstrong, J.F.; Faccenda, E.; Harding, S.D.; et al. The concise guide to pharmacology 2019/20: G protein-coupled receptors. *Br. J. Pharmacol.* **2019**, *176*, S21–S141. [[CrossRef](#)] [[PubMed](#)]